HHS Public Access

Author manuscript

*Science*. Author manuscript; available in PMC 2021 August 22.

Published in final edited form as:

*Science*. 2021 January 22; 371(6527): 405–410. doi:10.1126/science.abb2683.

# Glycolysis Fuels Phosphoinositide 3-Kinase Signaling to Bolster T Cell Immunity

**Ke Xu**[1,2], **Na Yin**[1,3], **Min Peng**[1,3], **Efstathios G. Stamatiades**[1], **Amy Shyu**[1,4], **Peng Li**[1], **Xian Zhang**[1], **Mytrang H. Do**[1,2], **Zhaoquan Wang**[1,2], **Kristelle J. Capistrano**[1], **Chun Chou**[1], **Andrew G. Levine**[1,2], **Alexander Y. Rudensky**[1,2,5], **Ming O. Li**[1,2,*]

[1]Immunology Program, Memorial Sloan Kettering Cancer Center, New York, NY 10065

[2]Immunology and Microbial Pathogenesis Graduate Program, Weill Cornell Graduate School of Medical Sciences, Cornell University, New York, NY 10065

[3]Current address: Institute for Immunology and School of Medicine, Tsinghua University, Beijing 100084, China

[4]Louis V. Gerstner Jr. Graduate School of Biomedical Sciences, Memorial Sloan Kettering Cancer Center, New York, NY 10065

[5]Howard Hughes Medical Institute, Memorial Sloan Kettering Cancer Center, New York, NY 10065

## Abstract

Infection triggers expansion and effector differentiation of T cells specific for microbial antigens in association with metabolic reprograming. Here, we show that the glycolytic enzyme lactate dehydrogenase A (LDHA) is induced in $CD8^+$ T effector cells via phosphoinositide 3-kinase (PI3K) signaling. In turn, ablation of LDHA inhibits PI3K-dependent phosphorylation of Akt and its transcription factor target Foxo1, causing defective antimicrobial immunity. LDHA deficiency cripples cellular redox control and diminishes ATP production in effector T cells, resulting in attenuated PI3K signaling. Thus, nutrient metabolism and growth factor signaling are highly integrated processes with glycolytic ATP serving as a rheostat to gauge PI3K-Akt-Foxo1 signaling in T cell immunity control. Such a bioenergetic mechanism for the signaling regulation may explain the century-old phenomenon known as the Warburg effect.

## One-Sentence Summary:

A PI3K and LDHA circuit enables T cell immunity.

*Correspondence to: lim@mskcc.org.

**Author Contributions:** M.O.L. conceived the project. K.X. designed and performed most experiments with input from M.O.L., N.Y., and M.P. K.X. and E.G.S. conducted the IF experiments. K.X. and A.S. performed cell sorting experiments. P.L., X.Z., M.H.D., Z.W., and C.C. assisted with the design of experiments. K.J.C. helped managing the mouse colony and A.G.L. and A.Y.R. provided critical mouse strains. K.X. wrote and M.O.L. edited the manuscript.

**Competing interests:** The authors declare no competing interests.

Supplementary Materials:
Materials and Methods
Figures S1–S17

In response to antigen stimulation, naïve T (Tn) cells differentiate into effector T (Teff) cells with rewired metabolic pathways (1–4). LDHA, a glycolysis enzyme that converts pyruvate to lactate, promotes Teff cytokine expression (5). However, glycolytic control of Teff responses to infection has yet to be defined, with a recent study questing its importance (6). To this end, we infected mice with *Listeria monocytogenes* expressing chicken ovalbumin protein as an antigen (LM-OVA) (7). H-2K$^{b}$-OVA$^{+}$ Teff cells expressed approximate five-fold higher LDHA than CD8$^{+}$ Tn cells (Fig. 1A and fig. S1). Activation of Tn cells with increasing doses of anti-CD3 progressively induced LDHA expression (Fig. 1B, fig. S2A and B), in line with induction of the LDHA transcriptional regulator c-Myc (Fig. 1B and fig. S2B) (8). Notably, although proximal T cell receptor (TCR) signaling, marked by phospho-Zap70 and phospho-LAT, was saturated at low concentration of anti-CD3 (fig. S2C), PI3K-dependent Akt phosphorylation showed a response curve similar to c-Myc and LDHA (Fig. 1B and fig. S2B). Indeed, blockade of PI3K signaling repressed c-Myc and LDHA expression (Fig. 1C and fig. S2D). By contrast, phospho-Zap70 and phospho-LAT were minimally affected (fig. S2E). These observations, together with previous findings that PI3K-Akt signaling promotes expression of the glucose transporter Glut1 (9), support a multifaceted role for PI3K in control of glucose metabolism in Teff cells.

To investigate LDHA function in Teff cells, we utilized *Tbx21*$^{Cre}$ mice that targeted H-2K$^{b}$-OVA$^{+}$ Teff cells (fig. S3A to C). *Ldha*$^{fl/fl}$ (designated as wild-type, WT) and *Tbx21*$^{Cre}$*Ldha*$^{fl/fl}$ (designated as knock-out, KO) mice were infected with LM-OVA followed by rechallenge, as protective immunity is dependent on T cells during a recall response (7). We found that KO mice had barely detectable antigen-specific Teff cells in contrast to robust expansion in WT mice (Fig. 1D). Defective T cell responses were observed throughout the course of bacterial infection (Fig. 1E), and pathogen was efficiently cleared in WT, but not KO, mice (Fig. 1F and fig. S3D to G). Similarly diminished expansion of Teff cells was observed in KO mice infected with lymphocytic choriomeningitis virus (fig. S4A and B). Furthermore, although WT Teff cells displayed a fully activated CD44$^{hi}$CD62L$^{lo}$ phenotype, KO Teff cells expressed high levels of CD62L (fig. S4C to F). LDHA deficiency also resulted in higher proportions of KLRG-1$^{lo}$CD127$^{hi}$ memory precursors effector cells (MPECs) at the expense of KLRG-1$^{hi}$CD127$^{lo}$ short-lived effector cells (SLECs) (fig. S4C to F) (10). Similar dysregulation of CD62L and KLRG1 was observed in Teff cells in KO mice infected with LM-OVA (fig. S5). Notably, attenuation of glucose metabolism with 2-deoxyd-glucose affected Teff cell expansion, but not CD62L or KLRG1 expression (fig. S5), revealing a qualitatively distinct function for LDHA in control of T cell activation and differentiation.

To probe CD8$^{+}$ T cell-intrinsic defects caused by LDHA deficiency, we crossed *Tbx21*$^{Cre}$*Ldha*$^{fl/fl}$ mice to the OT-I TCR-transgenic background. In a co-transfer setting, time-dependent out-competition of KO OT-I T cells by WT OT-I T cells was observed in association with diminished proliferation (fig. S6A, Fig. 2A and B). Mitochondrial reactive oxygen species (ROS) has been implicated in the control of T cell proliferation (11). Although WT OT-I T cells had higher levels of total ROS, mitochondrial ROS was higher in KO OT-I T cells (fig. S6B and C). This suggested that their diminished expansion was unlikely caused by defective mitochondrial activity. In addition, KO OT-I T cells expressed lower levels of effector molecules IFN-γ, TNF-α and granzyme B (fig. S7). Furthermore,

KO OT-I T cells failed to downregulate CD62L and differentiate to SLECs (Fig. 2C and fig. S8A). Thus, LDHA deficiency causes a multitude of T cell-intrinsic defects in activation, proliferation, and differentiation.

Teff cell heterogeneity is governed by growth factor signaling that modulates the transcriptional programs of T cells (12). Notably, the transcription factor Foxo1 promotes CD62L expression and MPEC generation (7, 13, 14), with its activity negatively regulated by Akt-induced phosphorylation (15, 16). Indeed, diminished phosphorylation of Akt and Foxo1 was observed in KO OT-I T cells (Fig. 2D and fig. S8B). In addition, defective phosphorylation of the mTORC1 target S6 was observed in KO OT-I T cells (fig. S8C). However, this would be unlikely to account for the severe defects of LDHA-deficient T cells, as ablation of mTORC1 causes an approximate two-fold reduction of antigen-specific T cells (17). To determine whether compromised Akt-induced Foxo1 phosphorylation might account for Teff cell defects observed in KO mice, we used a mouse strain expressing a phosphorylation-resistant form of Foxo1 (Fig. 2E and fig. S9A) (18). Compared to WT mice, *Tbx21*$^{Cre}$*Foxo1*$^{AAA/+}$ mice had barely detectable H-2K$^{b}$-OVA$^{+}$ Teff cells, which also failed to downregulate CD62L or upregulate KLRG-1 (Fig. 2F and fig. S9B to D). Thus, LDHA promotes Akt-Foxo1 signaling in CD8$^{+}$ Teff cells with ectopic activation of Foxo1 recapitulating the defects associated with LDHA deficiency.

To determine whether LDHA broadly promoted Akt-Foxo1 signaling in CD8$^{+}$ T cells, we crossed *Ldha*$^{fl/fl}$ mice with *Cd4*$^{Cre}$ mice to delete *Ldha* in Tn cells (Fig. 3A). Notably, LDHA deficiency had negligible effects on Akt-Foxo1 signaling in Tn cells; yet, activated KO T cells had diminished Akt and Foxo1, but not Zap70 or LAT, phosphorylation (Fig. 3B and fig. S10A), which was recapitulated with a LDHA inhibitor in WT T cells (fig. S10B). LDHA-catalyzed pyruvate to lactate conversion defines an efficient pathwayof carbon disposal with its deficiency predicted to diminish glycolysis-associated ATP production. Indeed, phosphorylation of the cellular energy sensor AMPKα (19) was higher in KO Teff cells (Fig. 3B and fig. S10A), in association with reduced ATP levels and glucose usage (fig. S11A and B).

To investigate whether reduced ATP production in antigen-experienced KO T cells accounted for diminished Akt-Foxo1 signaling, we restored ATP with streptolysin O (SLO) (fig. S11C and D) (20). As expected, anti-CD3/CD28-induced Akt and Foxo1 phosphorylation was inhibited in the absence of LDHA, which was unaltered by the addition of ATP (Fig. 3C and fig. S11E). SLO alone inhibited Akt and Foxo1 phosphorylation; by contrast ATP supplementation together with SLO enhanced Akt-Foxo1 signaling and corrected the defects associated with LDHA deficiency (Fig. 3C and fig. S11E). As the proximal TCR signaling was unaffected (fig. S12), we examined whether the differential bioenergetic states impacted the generation of PI3K-catalized phosphatidylinositol (3,4,5)-trisphosphate (PIP3), a rate-limiting step for PDK1-mediated Akt phosphorylation (21). Indeed, KO T cells produced lower amounts of PIP3, which was unaffected by ATP supplementation (Fig. 3D). Inclusion of SLO in the absence or presence of ATP inhibited or enhanced PIP3 generation, respectively, nullifying the differences between WT and KO T cells (Fig. 3D). Similar to murine T cells, blockade of LDHA-mediated aerobic glycolysis almost completely inhibited Akt-Foxo1 signaling in antigen-experienced human T cells,

which could be corrected by SLO-assisted intracellular delivery of ATP (fig. S13). These observations reveal an evolutionarily conserved ATP-sensing property of the PI3K pathway.

LDHA-catalyzed conversion of pyruvate to lactate regenerated cytosolic oxidized nicotinamide adenine dinucleotide ($NAD^+$) to support glycolytic ATP generation (Fig. 4A). Indeed, the $NAD^+$/NADH ratio was lower in activated KO T cells (Fig. 4B), in association with a lower extracellular acidification rate (ECAR), but a higher oxygen consumption rate (OCR) (Fig. 4C, fig. S14A and B). The mitochondrial electron transport chain (ETC)-mediated oxygen reduction promotes ATP synthesis through oxidative phosphorylation as well as glycolysis when coupled with redox shuttle systems (Fig. 4A and fig. S14C). To delineate contribution of these ETC-dependent sources of ATP to Akt-Foxo1 signaling, we utilized an ATP synthase inhibitor oligomycin and an uncoupler FCCP (Fig. 4C–D and fig. S14C). Oligomycin attenuated Akt and Foxo1 phosphorylation in WT T cells, whereas Akt-Foxo1 signaling in KO T cells was barely detectable (Fig. 4E and fig. S14D). Notably, treatment with FCCP or oligomycin plus FCCP enhanced Akt-Foxo1 signaling in WT T cells in an ETC-dependent manner, but not in KO T cells (Fig. 4E, fig. S14D and S15), in agreement with their higher spare respiratory capacity (SRC) (Fig. 4C). In contrast to activated T cells, WT and KO Tn cells exhibited comparable ECAR and OCR (fig. S16A to C), and oligomycin or FCCP inhibited Akt and Foxo1 phosphorylation (fig. S16D). Thus, Akt-Foxo1 signaling is supported by mitochondrial and glycolytic ATP in Tn and Teff cells, respectively. Furthermore, glycolytic ATP production is enabled primarily by LDHA with ETC playing a subsidiary role (fig. S17).

Antigen stimulation of $CD8^+$ T cells induces glucose uptake to support effector functions (8, 22–25). A selective role for glycolytic ATP to fuel PI3K signaling in Teff cells can be consequent to remodeling of the mitochondrial network (26), which may spare it as an energy house for glucose anabolism including acetyl-CoA-mediated gene regulation (5). Diminished glycolytic ATP production in LDHA-deficient Teff cells impairs PI3K, but not proximal TCR signaling. Notably, Zap70 has an ATP Km around 3 μM (27), whereas PI3Kδ, the major isoform expressed in T cells, has an ATP Km around 118 μM (28), which may render PI3Kδ to function as an ATP sensor in gauging the bioenergetic state of Teff cells. As enhanced PI3K signaling is a major oncogenic event (29), future studies will uncover whether the PI3K-LDHA positive feedback circuit provides a mechanistic explanation for the Warburg effect that is observed in cancer cells (30). Such a bioenergetic mechanism for the regulation of signaling may also guide the development of effective vaccines for infectious diseases and therapeutics for cancer.

## Supplementary Material

Refer to Web version on PubMed Central for supplementary material.

## Acknowledgments:

The authors thank members of the Li laboratory and Morgan Huse for helpful discussions.

**Funding:**

This work was supported by the National Institutes of Health (R01 AI 102888 to M.O.L.), the Howard Hughes Medical Institute (Faculty Scholar Award to M.O.L.), and the Memorial Sloan Kettering Cancer Center Support Grant/Core Grant (P30 CA08748).

## Data and materials availability:

All data is available in the main text or the supplementary materials. All materials used in the research are available upon request.

## References:

1. Wang R, Green DR, Metabolic checkpoints in activated T cells. Nat Immunol13, 907–915 (2012). [PubMed: 22990888]
2. MacIver NJ, Michalek RD, Rathmell JC, Metabolic regulation of T lymphocytes. Annu Rev Immunol31, 259–283 (2013). [PubMed: 23298210]
3. Chapman NM, Boothby MR, Chi H, Metabolic coordination of T cell quiescence and activation. Nat Rev Immunol20, 55–70 (2020). [PubMed: 31406325]
4. Pearce EL, Poffenberger MC, Chang CH, Jones RG, Fueling immunity: insights into metabolism and lymphocyte function. Science342, 1242454 (2013). [PubMed: 24115444]
5. Peng Met al., Aerobic glycolysis promotes T helper 1 cell differentiation through an epigenetic mechanism. Science354, 481–484 (2016). [PubMed: 27708054]
6. Ma EHet al., Metabolic Profiling Using Stable Isotope Tracing Reveals Distinct Patterns of Glucose Utilization by Physiologically Activated CD8+ T Cells. Immunity, (2019).
7. Kim MV, Ouyang W, Liao W, Zhang MQ, Li MO, The transcription factor Foxo1 controls central-memory CD8+ T cell responses to infection. Immunity39, 286–297 (2013). [PubMed: 23932570]
8. Wang Ret al., The transcription factor Myc controls metabolic reprogramming upon T lymphocyte activation. Immunity35, 871–882 (2011). [PubMed: 22195744]
9. Wofford JA, Wieman HL, Jacobs SR, Zhao Y, Rathmell JC, IL-7 promotes Glut1 trafficking and glucose uptake via STAT5-mediated activation of Akt to support T-cell survival. Blood111, 2101–2111 (2008). [PubMed: 18042802]
10. Joshi NSet al., Inflammation directs memory precursor and short-lived effector CD8(+) T cell fates via the graded expression of T-bet transcription factor. Immunity27, 281–295 (2007). [PubMed: 17723218]
11. Sena LAet al., Mitochondria are required for antigen-specific T cell activation through reactive oxygen species signaling. Immunity38, 225–236 (2013). [PubMed: 23415911]
12. Kaech SM, Cui W, Transcriptional control of effector and memory CD8+ T cell differentiation. Nat Rev Immunol12, 749–761 (2012). [PubMed: 23080391]
13. Rao RR, Li Q, Gubbels Bupp MR, Shrikant PA, Transcription factor Foxo1 represses T-bet-mediated effector functions and promotes memory CD8(+) T cell differentiation. Immunity36, 374–387 (2012). [PubMed: 22425248]
14. Hess Michelini R, Doedens AL, Goldrath AW, Hedrick SM, Differentiation of CD8 memory T cells depends on Foxo1. J Exp Med210, 1189–1200 (2013). [PubMed: 23712431]
15. Ouyang W, Li MO, Foxo: in command of T lymphocyte homeostasis and tolerance. Trends Immunol32, 26–33 (2011). [PubMed: 21106439]
16. Hedrick SM, Hess Michelini R, Doedens AL, Goldrath AW, Stone EL, FOXO transcription factors throughout T cell biology. Nat Rev Immunol12, 649–661 (2012). [PubMed: 22918467]
17. Pollizzi KNet al., mTORC1 and mTORC2 selectively regulate CD8(+) T cell differentiation. J Clin Invest125, 2090–2108 (2015). [PubMed: 25893604]
18. Ouyang Wet al., Novel Foxo1-dependent transcriptional programs control T(reg) cell function. Nature491, 554–559 (2012). [PubMed: 23135404]
19. Rolf Jet al., AMPKalpha1: a glucose sensor that controls CD8 T-cell memory. Eur J Immunol43, 889–896 (2013). [PubMed: 23310952]

20. Walev Iet al., Delivery of proteins into living cells by reversible membrane permeabilization with streptolysin-O. Proc Natl Acad Sci U S A98, 3185–3190 (2001). [PubMed: 11248053]
21. Costello PS, Gallagher M, Cantrell DA, Sustained and dynamic inositol lipid metabolism inside and outside the immunological synapse. Nat Immunol3, 1082–1089 (2002). [PubMed: 12389042]
22. Cham CM, Gajewski TF, Glucose availability regulates IFN-gamma production and p70S6 kinase activation in CD8+ effector T cells. J Immunol174, 4670–4677 (2005). [PubMed: 15814691]
23. Gubser PMet al., Rapid effector function of memory CD8+ T cells requires an immediate-early glycolytic switch. Nat Immunol14, 1064–1072 (2013). [PubMed: 23955661]
24. Ho PCet al., Phosphoenolpyruvate Is a Metabolic Checkpoint of Anti-tumor T Cell Responses. Cell162, 1217–1228 (2015). [PubMed: 26321681]
25. Menk AVet al., Early TCR Signaling Induces Rapid Aerobic Glycolysis Enabling Distinct Acute T Cell Effector Functions. Cell Rep22, 1509–1521 (2018). [PubMed: 29425506]
26. Buck MDet al., Mitochondrial Dynamics Controls T Cell Fate through Metabolic Programming. Cell166, 63–76 (2016). [PubMed: 27293185]
27. Isakov N, Wange RL, Watts JD, Aebersold R, Samelson LE, Purification and characterization of human ZAP-70 protein-tyrosine kinase from a baculovirus expression system. J Biol Chem271, 15753–15761 (1996). [PubMed: 8663155]
28. Somoza JRet al., Structural, biochemical, and biophysical characterization of idelalisib binding to phosphoinositide 3-kinase delta. J Biol Chem290, 8439–8446 (2015). [PubMed: 25631052]
29. Goncalves MD, Hopkins BD, Cantley LC, Phosphatidylinositol 3-Kinase, Growth Disorders, and Cancer. N Engl J Med379, 2052–2062 (2018). [PubMed: 30462943]
30. Warburg O, The Metabolism of Carcinoma Cells. The Journal of Cancer Research9, 148–163 (1925).
31. Levine AGet al., Stability and function of regulatory T cells expressing the transcription factor T-bet. Nature546, 421–425 (2017). [PubMed: 28607488]

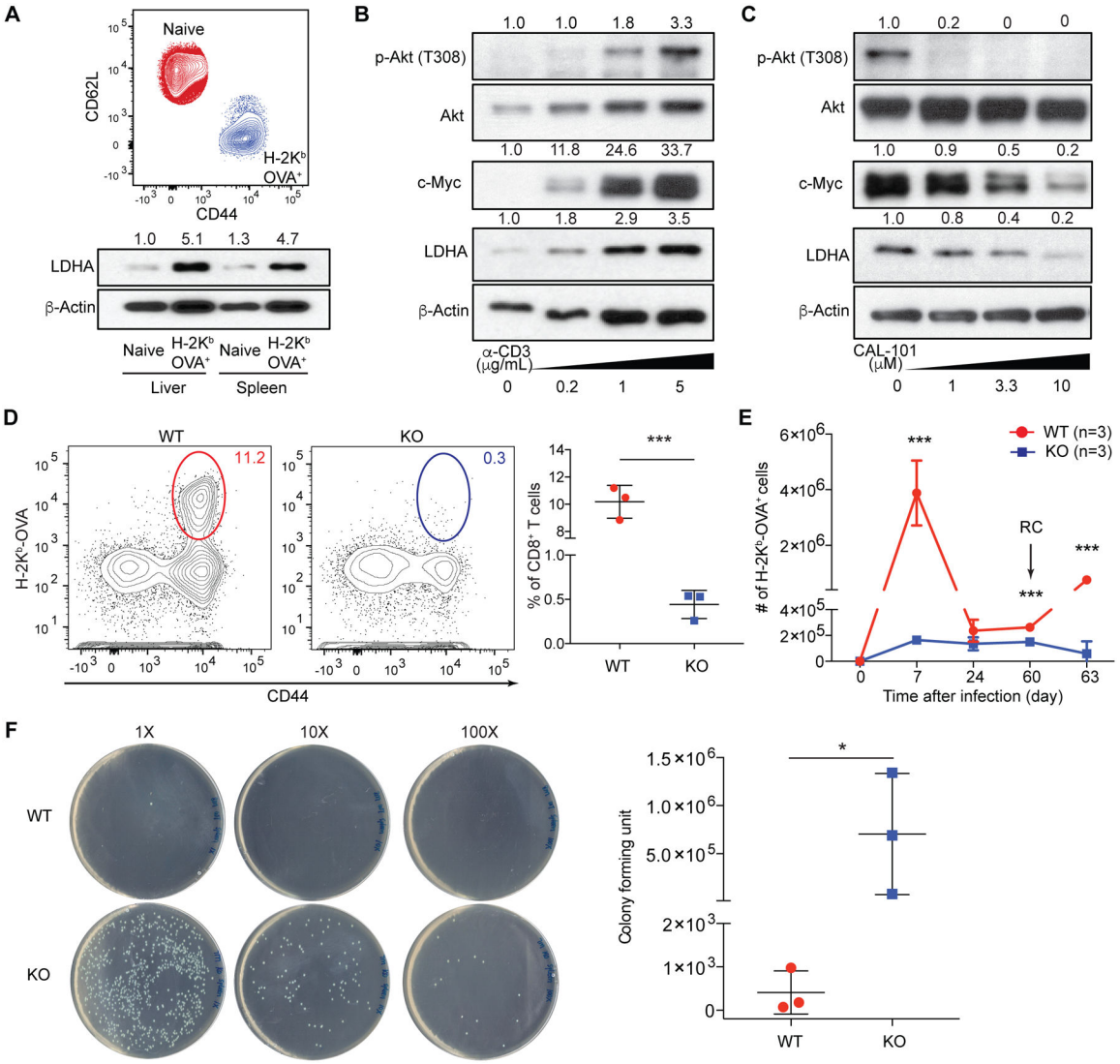


**Fig. 1. PI3K-dependent expression of LDHA in CD8$^+$ effector T cells is essential for antibacterial immunity**

(**A**) Flow cytometric analysis of CD44 and CD62L expression in splenic naïve and H-2K$^b$-OVA$^+$ CD8$^+$ T cells 7 days post LM-OVA infection. Immunoblotting and normalized expression of LDHA to β-actin. (**B**) Naïve CD8$^+$ T cells were stimulated with anti-CD3 in the presence of anti-CD28, and IL-2. Immunoblotting and normalized expression of p-Akt (T308) to Akt as well as c-Myc and LDHA to β-actin. (**C**) Naïve CD8$^+$ T cells were stimulated with anti-CD3, anti-CD28, and IL-2 in the presence of the PI3K inhibitor, CAL-101. Immunoblotting and normalized expression of p-Akt (T308) to Akt as well as c-Myc and LDHA to β-actin. (**D** to **F**) *Ldha*$^{fl/fl}$ (wild-type, WT) and *Tbx21*$^{Cre}$*Ldha*$^{fl/fl}$ (knockout, KO) mice were infected followed or not by re-challenge (RC) with LM-OVA. (**D**) Representative flow cytometry plots and frequencies of splenic H-2K$^b$-OVA$^+$ CD8$^+$ T cells 7 days post LM-OVA infection. (**E**) H-2K$^b$-OVA$^+$ CD8$^+$ T cells were enumerated 7, 24, 60 days post-infection, and day-3 post-secondary infection. (**F**) Splenic bacterial burden from day-3-RC mice. Data are representative of three (**A** to **C**) and two (**D** to **F,** n= 3

per genotype, mean ± SD) independent experiments. Unpaired *t* tests for the measurements between the two groups (**D** and **F**) and multiple *t* tests between the two groups (**E**): *$p<0.05$ and ***$p<0.001$.

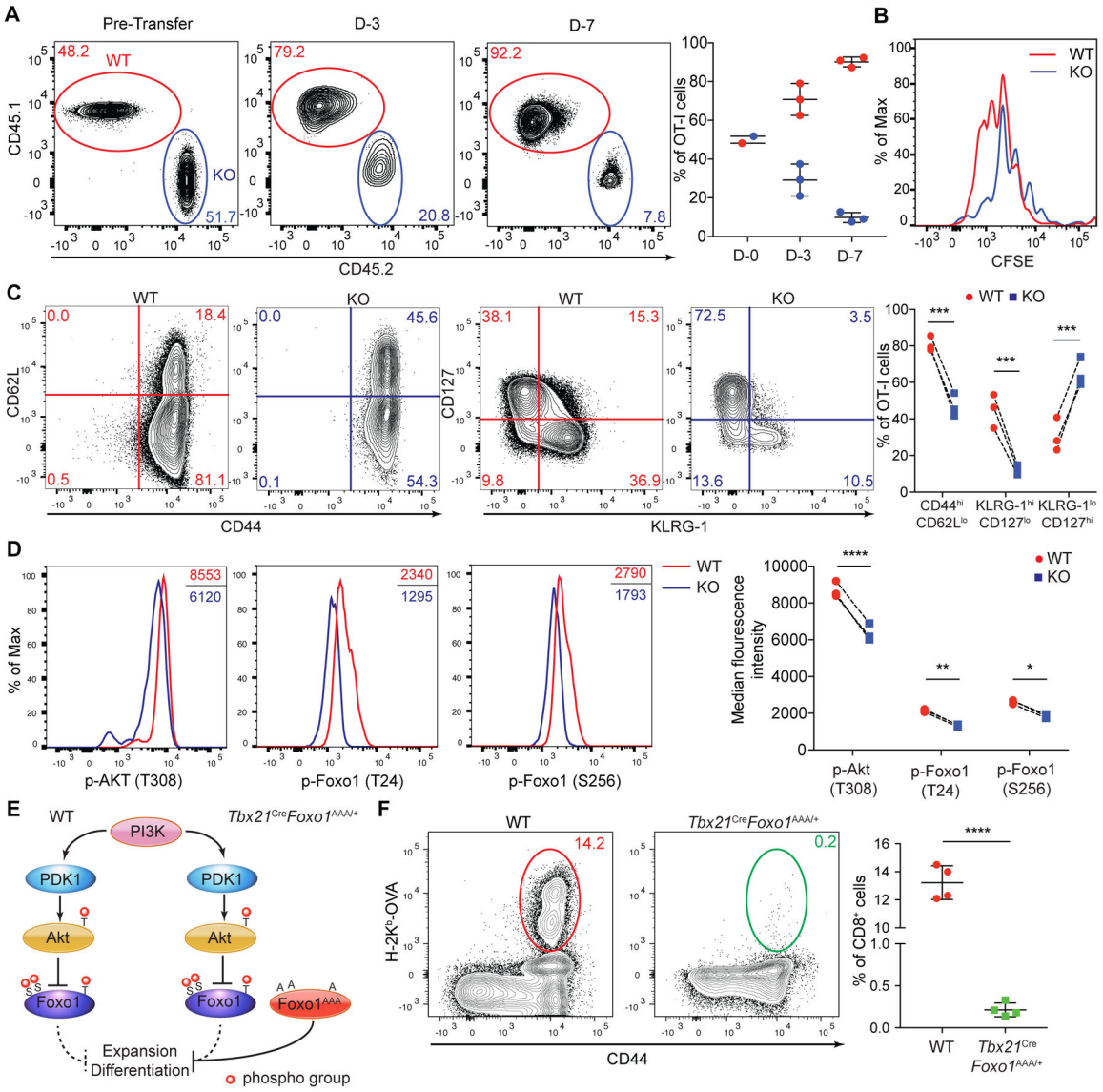


**Fig. 2. LDHA deficiency impairs Akt and Foxo1 phosphorylation causing defective CD8$^+$ T cell expansion and differentiation**

(**A** to **D**) Congenically marked naïve *Ldha*$^{fl/fl}$ (wild-type, WT) and *Tbx21*$^{Cre}$*Ldha*$^{fl/fl}$ (knockout, KO) OT-I T cells were CFSE-labeled, mixed at a 1:1 ratio and transferred into wild-type recipient mice followed by infection with LM-OVA. (**A**) Representative plots and ratios (mean ± SD) of splenic WT and KO OT-I T cells day-3 and day-7 post-infection. (**B**) Proliferation of splenic WT and KO OT-I T cells at day-3 post-infection was assessed by CFSE dilution. (**C**) Representative flow cytometry plots of CD44, CD62L, CD127, and KLRG-1 expression and the percentages of CD44$^{hi}$CD62L$^{lo}$, KLRG-1$^{hi}$CD127$^{lo}$, and KLRG-1$^{lo}$CD127$^{hi}$ populations among splenic WT and KO OT-I T cells from recipient mice day-7 post-infection. (**D**) Representative flow cytometry plots and median florescence intensities of p-Akt (T308), p-Foxo1 (T24), and p-Foxo1 (S256) in splenic WT and KO OT- I T cells. (**E**) A schematic of the PI3K-Akt-Foxo1 signaling pathway. *Foxo1*$^{AAA}$ was engineered to resist AKT-mediated repression by replacing three phosphorylation sites T24,

S256, and S319 with alanine (A). (**F**) Representative flow cytometry plots and frequencies of splenic H-2K$^{b}$-OVA$^{+}$ CD8$^{+}$ T cells in WT and *Tbx21*$^{Cre}$*Foxo1*$^{AAA/+}$ mice 7 days post LM-OVA infection (n=4 per genotype, mean ± SD). Data are representative of at least three independent experiments (**A** to **F**). Paired *t* tests for the measurements between the two groups (**C** and **D**) and unpaired *t* test for the measurements between the two groups (**F**): **p*<0.05, ***p*<0.01, ****p*<0.001, and *****p*<0.0001.

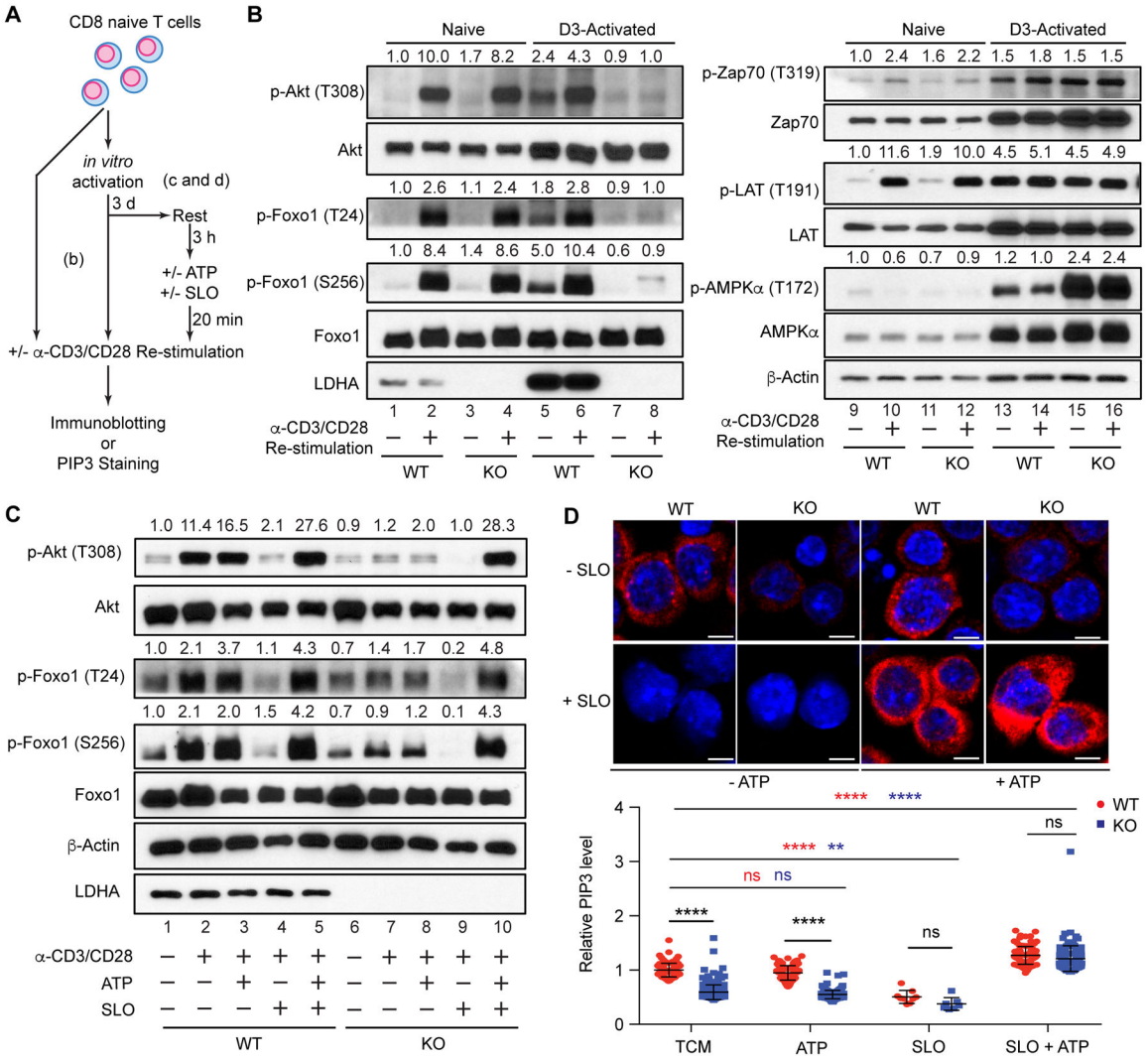


**Fig. 3. Reduced glycolytic ATP production accounts for defective PI3K-Akt-Foxo1 signaling in LDHA-deficient T cells following antigen stimulation**

(**A**) A schematic depicting how naïve CD8$^+$ T cells were treated for assessment of kinase signaling and PIP3 generation. (**B**) Naïve *Ldha*$^{fl/fl}$ (wild-type, WT) and *Cd4*$^{Cre}$*Ldha*$^{fl/fl}$ (knockout, KO) CD8$^+$ T cells were stimulated with anti-CD3, anti-CD28, and IL-2 for 3 days. Day-3 activated T cells and freshly isolated naïve WT and KO CD8$^+$ T cells were left untreated, or labeled with biotinylated anti-CD3 and anti-CD28 and activated by streptavidin crosslinking. Immunoblotting and normalized expression of p-Akt (T308) to Akt, p-Foxo1 (T24) or p-Foxo1 (S256) to Foxo1, p-Zap70 (T319) to Zap70, p-LAT (T191) to LAT, and p-AMPKα (T172) to AMPKα. (**C**) Day-3 activated WT and KO CD8$^+$ T cells were collected, rested in RPMI-1640 medium, and incubated in the absence or presence of ATP and/or Streptolysin O (SLO). T cells were subsequently restimulated with biotinylated anti-CD3 and anti-CD28 through streptavidin crosslinking. Immunoblotting and normalized expression of p-Akt (T308) to Akt, and p-Foxo1 (T24) or p-Foxo1 (S256) to Foxo1. (**D**) Representative immunofluorescent images of PIP3 and its quantification in WT and KO CD8$^+$ T cells after receiving the indicated treatments as described in (**C**). Each

dot represents one cell and the scale bar represents 5 micrometers. Data are representative of three (**A** to **C**) or two (**D**) independent experiments. Two-way ANOVA test for the measurements between the two groups (**D**): $^{**}p<0.01$ and $^{****}p<0.0001$.

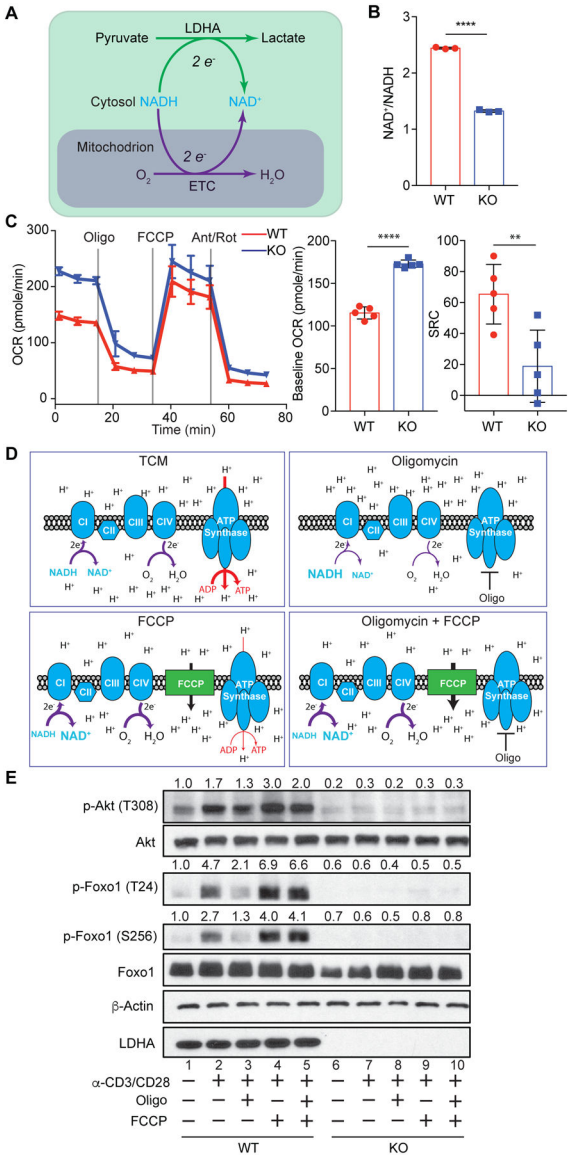


**Fig. 4. Mitochondrial respiration, but not ATP production, promotes Akt-Foxo1 signaling in activated T cells**

(**A**) A schematic depicting electron transfer and disposition by cytosolic LDHA and mitochondrial electron transport chain (ETC) associated with NADH to $NAD^+$ conversion. (**B**) Naïve *Ldha*$^{fl/fl}$ (wild-type, WT) and *Cd4*$^{Cre}$*Ldha*$^{fl/fl}$ (knockout, KO) $CD8^+$ T cells were stimulated with anti-CD3, anti-CD28, and IL-2 for 3 days. The amounts of NADH and $NAD^+$ were measured. The ratios of $NAD^+$ over NADH are plotted. (**C**) Measurements and quantifications of oxygen consumption rate (OCR) and spared respiratory capacity (SRC) of day-3 activated WT and KO $CD8^+$ T cells. Sequential chemical treatments are indicated as shown in the graph. Oligo: oligomycin; FCCP: Trifluoromethoxy carbonylcyanide phenylhydrazone; Ant: antimycin; Rot: rotenone. (n=5 per genotype, mean ± SD) (**D**) A schematic of mitochondrial ETC, proton distribution, and ATP synthetase activity under the indicated treatment conditions. (**E**) Day-3 activated WT and KO $CD8^+$ T cells were collected, and incubated in RPMI-1640 medium in the absence or presence of oligomycin

and/or FCCP. T cells were subsequently restimulated with biotinylated anti-CD3 and anti-CD28 through streptavidin crosslinking. Immunoblotting and normalized expression of p-Akt (T308) to Akt, and p-Foxo1 (T24) or p-Foxo1 (S256) to Foxo1. Data are representative of three independent experiments (**B**, **C** and **E**). Unpaired *t* tests for the measurements between the two groups (**B** and **C**): ** $p<0.01$ and **** $p<0.0001$.